PCCP

PAPER

View Article Online
View Journal | View Issue

Cite this: *Phys. Chem. Chem. Phys.*, 2019, **21**, 19816

Optical spectra of molecular aggregates and crystals: testing approximation schemes†

M. Anzola, F. Di Maiolo and A. Painelli *

The interplay between exciton delocalization and molecular vibrations profoundly affects optical spectra of molecular aggregates and crystals. The exciton motion occurs on a similar timescale as molecular vibrations, leading to a complex and intrinsically non-adiabatic problem that has been handled over the years introducing several approximation schemes. Here we discuss systems where intermolecular distances are large enough so that only electrostatic intermolecular interactions enter into play and can be treated in the dipolar approximation. Moreover, we only account for interactions between transition dipole moments, as relevant to symmetric molecules, with negligible permanent (multi)polar moments in the ground and low-lying excited states. Translational symmetry is fully exploited to obtain numerically exact solutions of the relevant Hamiltonian for systems of comparatively large size. This offers a unique opportunity to assess the reliability of different approximation schemes. The so-called Heitler–London approximation, only accounting for the effects of intermolecular interactions among degenerate electronic states, leads to the celebrated exciton model, widely adopted to describe optical spectra of molecular aggregates and crystals. We demonstrate that, mainly due to a cancellation of errors, the exciton model approximates well the position of exciton bands and reasonably well the bandshapes, but it fails to predict spectral intensities, leading to underestimated intensities in J-aggregates and overestimated intensities in H-aggregates. This general result is validated against an exact sum-rule. Finally, we address the validity of several approximation schemes adopted to reduce the dimension of the vibrational basis.

Received 2nd June 2019,
Accepted 27th August 2019

DOI: 10.1039/c9cp03122g

rsc.li/pccp

1 Introduction

Molecular materials are characterized by intermolecular forces much weaker than the chemical bonds inside each individual molecular unit. In spite of that, in molecular materials intermolecular interactions deeply affect optical spectra, that therefore cannot be calculated as the sum of molecular spectra. Intermolecular charge transfer (CT) was early recognized as a source of impressive spectroscopic phenomena in absorption spectra of molecular materials, both in the visible and near-IR spectral regions, where so-called CT absorption bands appear.[1,2] Vibrational spectra are also affected by CT, with the appearance of strong features due to large charge fluxes driven by molecular vibrations or lattice modes (phonons).[3–6] In molecular materials with intermolecular distances larger than the sum of van der Waals radii, electrons are localized within each molecular unit and CT interactions are absent. Even in these conditions, electrostatic intermolecular interactions may have prominent effects, driving resonance energy transfer among different molecular species[7–9] and energy delocalization among equivalent (or nearly so) molecules in molecular crystals and aggregates.[10–12]

The physics of excitons and of optical spectra in molecular crystals was first addressed in the seminal works of Craig,[13] Davidov[14] and Agranovich.[15] The same physics also applies to molecular aggregates: the ground-breaking discovery of the anomalous spectra of cyanine aggregates[16] opened the research field of molecular aggregates, with the seminal theoretical work of Kasha.[17] An enormous body of experimental and theoretical work can be found in the literature, as extensively reviewed by Spano.[11,12] Current understanding of optical spectra of molecular aggregates and crystals is mainly based on the so-called exciton model that, only accounting for electrostatic interactions among degenerate states, leads to a large reduction of the basis set. Along these lines, analytical solutions have been obtained of the electronic problem that offer a reliable basis for understanding spectral properties of molecular aggregates and crystals. The approximations of the exciton model were discussed in the original papers[14,15] and have been recently addressed in relation with aggregates of polarizable molecules with polar[18–20] or quadrupolar character.[21–24]

Molecular vibrations add another layer of complexity to the physics of molecular aggregates and crystals: the deformation of the molecular structure upon excitation is responsible for the

Department of Chemistry, Life Science and Environmental Sustainability, Università di Parma, 43124 Parma, Italy. E-mail: anna.painelli@unipr.it

† Electronic supplementary information (ESI) available. See DOI: 10.1039/c9cp03122g

Franck–Condon structure of absorption and fluorescence spectra of isolated molecules in solution, but the shape of absorption and fluorescence spectra of molecular aggregates often largely deviates from the Franck–Condon behavior,[11,25] as first recognized in the narrow and structureless absorption and emission spectra of aggregates of cyanine dyes.[16] Delocalization energies and vibrational energies are often comparable in molecular aggregates and the adiabatic approximation must be abandoned. Treating the electronic and vibrational degrees of freedom on the same foot is a formidable task. Indeed analytical solutions of the coupled electronic and vibrational problem are available for an infinite one-dimensional array of molecules in the exciton approximation and accounting for a single coupled vibration.[25,26] Most often approximations schemes have been proposed to treat the problem, whose validity and applicability need a careful discussion.

In this paper we critically review the approximation schemes for the simplest model of molecular aggregates that, only addressing intermolecular interactions between transition dipole moments, applies to aggregates and crystals of non-polar (centrosymmetric) molecules, and, more precisely to molecules whose permanent dipole moments in the ground and low-lying excited states are negligible, much as their quadrupolar and higher order moments in the multipolar expansion. Accordingly, the model does not apply to so-called charge-transfer dyes, *i.e.*, π-conjugated molecules with electron-donor and acceptor groups. Model for aggregates of polar[18,20] and quadrupolar dyes,[22–24,27] have been proposed recently.

2 The model

We consider a one-dimensional array of equivalent molecules. Only two electronic states are available per molecule, the ground $|g\rangle$ and the excited state $|e\rangle$. The underlying hypothesis is that higher excited states are located at too large energies to be relevant. This restricts our model to large π-conjugated dyes, having the lowest excited state in the visible region of the spectrum, while higher excited states are in the ultraviolet region. Both the ground and the excited states have negligible dipolar and multipolar moments, so that the only relevant matrix element of the dipole moment operator is $\langle g|\hat{\mu}|e\rangle = \mu_0$. The magnitude of μ_0 is experimentally accessible from the oscillator strength of the g → e transition measured for the isolated dye in solution:[28]

$$f_{ge} = \frac{2}{3}\frac{m_e}{\hbar e^2}\omega_0\mu_0^2, \quad (1)$$

where m_e is the electron mass, e the electron charge and ω_0 the frequency of the g → e transition. Alternatively, the transition dipole moment can be obtained from quantum chemical calculations, with the added value of getting information about the dipole moment orientation.

A linear electron–vibration coupling model is adopted, introducing an internal vibrational coordinate $\hat{q}_i$ per molecule. The two electronic states of each molecule are described by two harmonic potential energy surfaces with the same frequency, ω_v, but displaced minima. The strength of the electron–vibration coupling is measured by the vibrational relaxation energy, λ, that, being related to the Huang–Rhys factor, $S = (\lambda/\hbar\omega_v)^2$, can be extracted from the analysis of the absorption or fluorescence bandshape of the isolated dye in solution.[28]

In the hypothesis that permanent polar and multipolar moments are negligible, the only surviving electrostatic intermolecular interactions are driven by transition dipole moments. The interaction between transition dipoles at i and j sites reads:[15]

$$J_{i,j} = \frac{\mu_0^2}{4\pi\varepsilon d_{ij}^3}D_{ij}, \quad (2)$$

where D_{ij} is a geometrical factor that only depends on the relative orientation of the transition dipole moments on sites i and j, while d_{ij} is the distance between the two molecular sites (see also ESI†). Finally, ε is the medium dielectric constant at optical frequencies (the squared refractive index). It accounts for the polarizability of the surrounding medium and includes the effects of electronic excitations not explicitly accounted for in the exciton model. In the following we will address one-dimensional molecular aggregates with one molecule per unit cell. To maintain translational symmetry we impose periodic boundary conditions, locating the N molecular units composing the aggregate at the vertices of a regular polygon as in Fig. 1, In these conditions intermolecular interactions only depend on the intermolecular distance and we define $J_m = J_{i,i\pm m}$. Two extreme cases will be considered: (a) nearest-neighbor interactions with $J_1 = J$ and $J_m = 0$ for $m > 1$; (b) long-range Coulomb interactions with $J_1 = J$ and $J_m = J[\sin(\pi/N)/\sin(m\pi/N)]^3$ for $m > 1$. In either case a single parameter, J, measuring the strength of the nearest-neighbor interaction, fully defines the model. Positive J (H aggregates, repulsive interactions) describe an aggregate where all molecular dipoles are aligned in a direction perpendicular to the plane of the polygon, while negative J (J aggregates, attractive interactions) correspond to the case where all dipoles are tangential to the polygon. The translational symmetry guaranteed by the adopted periodic boundary conditions and the absence of disorder are instrumental to reduce the dimension

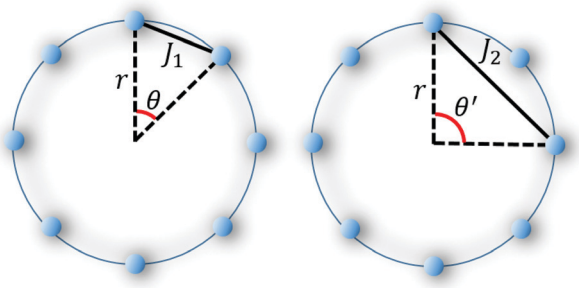

Fig. 1 A schematic view of a 8-site chain with periodic boundary conditions. In H aggregates the molecular units, represented in the figure as points, are oriented as to have the transition dipole moments aligned in a direction perpendicular to the plane of the polygon. In J aggregates the transition dipole moments are tangential to the polygon.

of the Hamiltonian matrices to be diagonalized, and are therefore very important to our approach. Of course these idealized conditions apply to large aggregates or crystals with a highly ordered structure and in the limit where the exciton correlation length is smaller than the actual dimension of the aggregates.

The Hamiltonian for a linear array of N molecules reads:[15]

$$\hat{H} = \sum_i \left[E - \lambda\left(\hat{a}_i^\dagger + \hat{a}_i\right)\right]\hat{n}_i + \hbar\omega_v \sum_i \left(\hat{a}_i^\dagger \hat{a}_i + \frac{1}{2}\right) + \sum_m J_m\left(\hat{b}_i^\dagger \hat{b}_{i+m} + \text{h.c.}\right) + \sum_m J_m\left(\hat{b}_i^\dagger \hat{b}_{i+m}^\dagger + \text{h.c.}\right), \quad (3)$$

where i and $i + m$ run on the N molecular sites. The operators $\hat{a}_i^\dagger$, $\hat{a}_i$ are the boson operators associated with the harmonic oscillator on site i. The operator $\hat{b}_i^\dagger$ creates an excitation on site i, by turning the molecule from state $|g\rangle$ to $|e\rangle$, while $\hat{b}_i$ destroys the excitation. As discussed by Agranovich,[29] these operators obey a Paulion algebra:

$$\left[\hat{b}_i, \hat{b}_j^\dagger\right] = \begin{cases} 1 - 2\hat{b}_j^\dagger \hat{b}_i, & \text{if } i = j \\ 0, & \text{if } i \neq j \end{cases}. \quad (4)$$

The first two terms in the Hamiltonian in eqn (3) describe the molecular problem, where E is the vertical excitation energy of the molecule in the aggregate. This energy may differ from $\hbar\omega_0$, the transition energy in the isolated molecule, due to local field effects, but we will neglect these corrections in the following, setting $E = \hbar\omega_0$. The last two terms account for intermolecular interactions: the same interaction J_m is responsible for the hopping of the excitation from site i to $i + m$ (and *vice versa*) and for the simultaneous creation (destruction) of two excitations on sites i and $i + m$.

The hopping term mixes states with the same number of excitons, *i.e.*, states having the same diagonal energy, while the last term in the above Hamiltonian describes the interaction among states whose energy differs by $2E$. Accordingly, the Heitler–London (HL) approximation is adopted in the common version of the exciton model (we will refer to it as the standard exciton model) neglecting all terms in the Hamiltonian mixing states with a different number of excitons.[15] The HL approximation, valid as long as J interactions are negligible with respect to E, leads to an enormous reduction of the basis set, since the problem can be solved inside subspaces with fixed number of excitations. In the HL approximation the ground state coincides with the vacuum electronic state $|\ldots ggg\ldots\rangle$ times the vacuum vibrational state (*i.e.*, the state where all molecular oscillators are in the vacuum state) and the excited state subspace of relevance to linear spectroscopy only contains the electronic manifold of the N states with a single exciton.

3 Exact diagonalization approach: calculating absorption and fluorescence spectra

When the last term in eqn (3) is non-negligible, it is not possible to factorize the problem as done in the standard exciton model. The complete basis can be obtained as the direct product of the 2^N electronic states times the vibrational basis, composed of the direct product of the states relevant to each one of the N harmonic oscillators. Of course, to make the problem numerically tractable the infinite vibrational basis must be truncated. In the following we will truncate the basis imposing a limit M_v to the total number of vibrational quanta in the aggregate, disregarding all states with $\sum_i \left\langle \hat{a}_i^\dagger \hat{a}_i \right\rangle > M_v$. Of course M_v must be large enough as to guarantee for converged and hence numerically exact results. The overall dimension of the vibrational basis is

$$n_v = \sum_{\nu=0}^{M_v} \binom{N + \nu - 1}{\nu}. \quad (5)$$

The electronic basis, of dimension 2^N can be truncated setting a limit to the number of excitons, disregarding states with $\sum_i \left\langle \hat{b}_i^\dagger b_i \right\rangle > M_e$. Again M_e must be chosen large enough to guarantee for convergence. In spite of the truncation, the dimension of the basis is too large to calculate optical spectra of aggregates with dimensions $N > 4$. To deal with larger systems we exploit translational symmetry.

In a system with periodic boundary conditions, translational symmetry guarantees for the conservation of the total (electronic + vibrational) wavevector, K. For a linear chain of N equivalent molecules the allowed K values in the first Brillouin zone are $K = \frac{2\pi}{N}s$, were s is an integer number in the $-\frac{N}{2} < s \leq \frac{N}{2}$ interval. Optical transitions conserve the total wavevector, so that, starting from the ground state ($K = 0$), only $K = 0$ excited states are reached upon absorption. According to the Kasha rule, emission always occurs from the lowest singlet excited state so that for J-aggregates $K = 0$ to $K = 0$ transitions are of interest. In H-aggregates the lowest excited states are located at $K = \frac{2\pi}{N}\max(s) = K_{max}$ so that only transitions from $K = K_{max}$ to $K = K_{max}$ are relevant, at least as long as temperature is low enough as not to populate excited states with different wavevectors.[12]

We implement the calculation using the bit-representation to store the basis set. One bit is needed to define the electronic state (either g or e) of each molecular site. Additional bits are needed for each molecule, to store the number of vibrational quanta in the relevant oscillator (we choose our basis with reference to the undisplaced harmonic oscillator relevant to the g state). Using three bits per molecule to store the vibrational information, we account for up to 7 vibrational quanta per molecule. Accordingly, we store each basis state in the computer memory as an integer number whose binary code is composed of 4 bits for each molecule in the aggregate, where the first bit represents the electronic state ($|0\rangle \equiv |g\rangle$, $|1\rangle \equiv |e\rangle$) and the following 3 bits store the integer number that counts the vibrational quanta. The basis set is created scrolling through all integer numbers from 0 to $16^N - 1$, and selecting only the states that comply with the required values of M_e and M_v.

Translational symmetry operations are then applied to the basis states to finally obtain symmetry-adapted linear combinations. Since the basis is very large, we do not store the full non-symmetrized basis, but we just store a single representative state for each symmetry-adapted linear combination together with the information concerning its multiplicity. The Hamiltonian in eqn (3) is finally written on the symmetrized basis and is diagonalized in the $K = 0$ and $K = K_{\max}$ subspaces for systems with up to $N = 7$ sites.

In a different strategy, as discussed in ref. 30, translational symmetry can be implemented by separately finding the wavevector for the electronic and vibrational states, k and q, respectively, and then combining the two wavevectors to give states with the required total wavevector. To this end, we transform the Paulion operators for creating/destroying an exciton to the Fourier space:

$$\hat{b}_j = \frac{1}{\sqrt{N}} \sum_k \mathrm{e}^{-ijk} \hat{b}_k, \quad \hat{b}_j^\dagger = \frac{1}{\sqrt{N}} \sum_k \mathrm{e}^{ijk} \hat{b}_k^\dagger, \tag{6}$$

and apply the same transformation to the boson operators that create/destroy vibrational quanta:

$$\hat{a}_j = \frac{1}{\sqrt{N}} \sum_q \mathrm{e}^{-ijq} \hat{a}_q, \quad \hat{a}_j^\dagger = \frac{1}{\sqrt{N}} \sum_q \mathrm{e}^{ijq} \hat{a}_q^\dagger. \tag{7}$$

The Hamiltonian in eqn (3) is rewritten using the transformed operators as follow:

$$\begin{aligned} \hat{H} \;=\; & \sum_k \hat{b}_k^\dagger \hat{b}_k \left(E + \sum_m J_m \mathrm{e}^{imk} \right) + \hbar\omega_{\mathrm{v}} \sum_q \hat{a}_q^\dagger \hat{a}_q \\ & - \frac{\lambda}{\sqrt{N}} \sum_{k,q} \left(\hat{a}_q^\dagger \hat{b}_k^\dagger \hat{b}_{k+q} + \hat{a}_{-q} \hat{b}_k^\dagger \hat{b}_{k+q} \right) \\ & + \frac{1}{2} \sum_{k,m} J_m \left(\hat{b}_k^\dagger \hat{b}_{-k}^\dagger \mathrm{e}^{imk} + \mathrm{h.c.} \right). \end{aligned} \tag{8}$$

The non-HL term (last term of the above equation) mixes up electronic states with different number of excitons and different k, making the symmetrization procedure cumbersome, so that, for the complete problem we prefer to go along the lines described above. In the HL approximation instead, the N electronic states with a single exciton are easily combined to give N linear combinations in the reciprocal space. The total wavevector K is calculated for each state as the sum of the electronic wavevector plus the vibrational contribution $K = k + \sum_q n_q q$, where n_q counts the number of vibrational quanta in the vibrational mode with wavevector q.

The symmetrized Hamiltonian is finally diagonalized in the relevant subspaces to get numerically exact non-adiabatic vibronic eigenstates that describe the combined electronic and vibrational motion in the aggregate. To calculate optical spectra we write the explicit expression for the dipole moment operator of the aggregate, and, considering aligned dipoles as to avoid vectorial sums, we get:

$$\hat{\mu} = \mu_0 \sum_i \left(\hat{b}_i^\dagger + \hat{b}_i \right) = \mu_0 \sqrt{N} \left(\hat{b}_{k=0}^\dagger + \hat{b}_{k=0} \right). \tag{9}$$

The linear absorption spectrum is finally calculated assigning a Gaussian lineshape to each transition:

$$\sigma(\omega) \propto \omega \sum_{\mathrm{E}} |\langle \mathrm{E}|\hat{\mu}|\mathrm{G}\rangle|^2 \mathrm{e}^{-\frac{1}{2}\frac{(\hbar\omega_{\mathrm{EG}} - \hbar\omega)^2}{\sigma^2}}, \tag{10}$$

where $\hbar\omega_{\mathrm{EG}}$ is the energy of the $|\mathrm{G}\rangle \rightarrow |\mathrm{E}\rangle$ transition.[31] We underline that in the standard exciton model, since the vacuum state $|\ldots \mathrm{ggg} \ldots\rangle$ is fully decoupled from states with one (or more) excitons, the eigenstates and hence the transition dipole moments are fully independent of the bare exciton frequency, ω_0. However, absorption spectra acquire a dependence on ω_0, or more precisely on the specific frequency of the electronic transitions, due to the ω prefactor in the above expression for linear absorbance.

The calculation of fluorescence spectra requires some care to single the long-lived state out of the excited states manifold. According to the Kasha rule, this state corresponds to the lowest excited state in the electronically excited manifold (we assume that temperature is low enough as to have a sizable population only on the lowest excited state). In the standard exciton model, since the Hamiltonian is diagonalized in the single-exciton manifold, the fluorescent state is easily recognized as the lowest energy state in the single-exciton manifold. Depending on the sign of intermolecular interactions the fluorescent state is found in either the $K = 0$ subspace ($J < 0$, J-aggregates) or in the $K = K_{\max}$ subspace ($J > 0$, H-aggregates). When relaxing the HL approximation, the eigenstates also contain the ground state vibrational manifold.[11] We therefore recognize the fluorescent state as the lowest energy state in either the $K = 0$ or $K_{\max}$ subspace with a number of excitons close to 1. The fluorescence spectrum is calculated as follows:[31]

$$I(\omega) \propto \omega^3 \sum_{\mathrm{E}} |\langle \mathrm{E}|\hat{\mu}|\mathrm{F}\rangle|^2 \mathrm{e}^{-\frac{1}{2}\frac{(\hbar\omega_{\mathrm{FE}} - \hbar\omega)^2}{\sigma^2}} \tag{11}$$

where $|\mathrm{F}\rangle$ is the fluorescent state and the sum runs on all eigenstates (including the ground state) having a lower energy and being located in the same subspace (either $K = 0$ or $K_{\max}$) as the fluorescent state. Since in the complete model the eigenstates also include the vibrational manifold of the ground state, eqn (11) can be used without further analysis. In the standard exciton model instead the $|\mathrm{E}\rangle$ states in the above equation corresponds to the vibrational eigenstates in the ground state manifold and must be explicitly written as the product of the electronic ground state $|\ldots \mathrm{ggg} \ldots\rangle$ (the zero exciton state, a state with $k = 0$) times the $q = 0$ or $q = K_{\max}$ states of the harmonic oscillators.

4 Exact results on finite size systems: validating the Heitler–London approximation

Fig. 2 shows selected results for typical model parameters. Specifically, we consider only nearest neighbor interactions (results for long-range Coulomb interactions can be found in the ESI†)

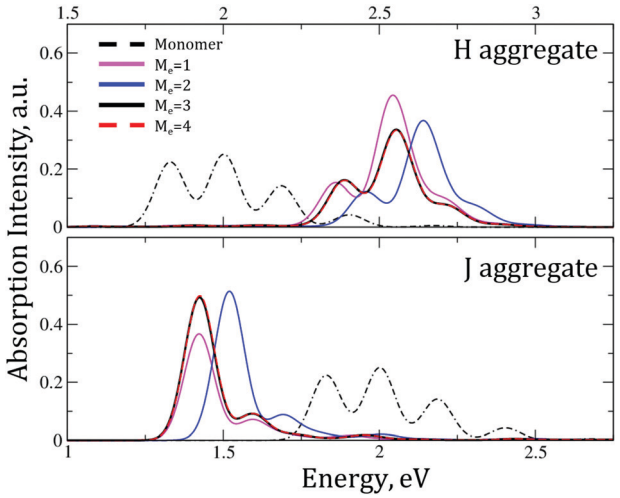

Fig. 2 Absorption spectra calculated for the complete Hamiltonian in eqn (3) only accounting for nearest neighbor interactions. Results are obtained for $N = 6$, $\hbar\omega_0 = 2.0$ eV, $\lambda = 0.17$ eV, $\hbar\omega_v = 0.17$ eV and $|J| = 0.255$ eV. The vibrational basis is truncated setting the maximum number of total vibrational quanta $M_v = 6$. The electronic basis is truncated fixing the maximum number of excitons M_e to a value ranging from 1 to 4. Results for $M_e = 1$ coincide with those obtained in the HL approximation. Top and bottom panels refer to H-aggregates ($J > 0$) and J-aggregates ($J < 0$), respectively.

for $\hbar\omega_0 = 2$ eV and $\hbar\omega_v = 0.17$ eV, corresponding to a system with an electronic excitation in the visible and a mid-IR vibrational mode. A medium-large vibrational coupling is considered, setting $\lambda = 0.17$ eV, corresponding to a monomer spectrum peaking at the 0–1 vibronic line (results for weaker and stronger coupling are also shown in the ESI†). The intermolecular interaction strength is fixed to $|J| = 0.255$ eV, roughly a tenth of the exciton bare energy, $\hbar\omega_0$. We estimate that this J value corresponds, for a typical oscillator strength $f = 1$ of the monomer, to an intermolecular distance $d \sim 7$ Å. The estimated distance would be reduced accounting for the medium dielectric constant ε in eqn (2). Results in the figure are obtained for $N = 6$, truncating the vibrational basis to $M_v = 6$, and refer to positive J (H-aggregates) in the upper panel and to negative J (J-aggregates) in the lower panel. Here and in the following intensity are shown per molecule. In each panel, the dash-dotted line shows the monomer spectrum and the continuous curves refer to results obtained truncating the number of excitons to $M_e = 1$–4, as specified in the legend. The first observation is that results for $M_e = 3$ and 4 are superimposed: accounting for up to 3 excitons leads to nominally exact results.

Results for $M_e = 1$ of course coincide with those obtained in the standard exciton model. Apparently the HL approximation works very well to estimate the position of the absorption band and reasonably well for the band-shape (small deviations are observed in H-aggregates), but it fails to reproduce the intensity of the spectrum. Calculated spectra show a non-monotonous behavior with increasing M_e: while for $M_e = 1$ the position of the absorption band is properly calculated (even if we are off with the intensity), $M_e = 2$ results are off with the frequency, but improve on the intensity. This immediately suggests that the HL approximation (corresponding to $M_e = 1$ results in the figure) gives good results for the band position due to error cancellation. The non-HL term in eqn (3) in fact mixes states with a number of excitons differing by 2: the energy of the ground state is lowered due to the non-HL mixing with two-exciton states by an amount similar to the stabilization of one-exciton states due to the mixing with the three-exciton states. Accordingly, the frequency of the observed transition is marginally affected by the non-HL terms. Of course the transition frequency calculated for $M_e = 2$ is overestimated since it accounts for the stabilization of the ground state, but not for stabilization of the excited states.

Spectra calculated in the HL approximation overestimate the intensity of H-aggregates and underestimate the intensity of J-aggregates. This interesting result deserves some discussion. Since in the HL approximation the excited states reached upon absorption are linear combinations of one-exciton states, the total squared transition dipole moment in an aggregate of N molecules is equal to the total squared transition dipole moment of N non-interacting molecules. This immediately points to an internal inconsistency of the exciton model in its standard implementation. As it is well known (see also the detailed analysis in the ESI†), the total oscillator strength of a system can always be related to a ground state property:

$$F = \sum_E f_{EG} = \frac{2}{3}\frac{m_e}{\hbar e^2}\sum_E \omega_{EG}\mu_{EG}^2 = -\frac{im_e}{3\hbar e^2}\langle G|[\hat{\mu},\hat{v}]|G\rangle, \quad (12)$$

where i is the imaginary unit and the velocity dipole operator, $\hat{v}$ is defined as:

$$i\hbar\hat{v} = [\hat{\mu},\hat{H}]. \quad (13)$$

In the HL approximation the aggregate ground state is the same as the ground state of N non-interacting monomers, so that the sum-rule in eqn (12) would impose the conservation of the total oscillator strength (per molecule) when going from the monomer to the aggregate. However, in the HL approximation the total dipole moment is conserved. Therefore in the standard exciton model the oscillator strength for J-aggregates (having a red-shifted transition with respect to the monomer) is underestimated, while it is overestimated for H-aggregates (having a blue-shifted absorption).

Of course the sum rule is strictly obeyed in the complete exciton model. Specifically, the commutator in eqn (12) is (see the derivation in the ESI†):

$$[\hat{\mu},\hat{v}] = \frac{1}{i\hbar}\mu_0^2\sum_i\left[\hbar\omega_0 - \lambda\left(\hat{a}_i^\dagger + \hat{a}_i\right)\right](4\hat{n}_i - 2), \quad (14)$$

so that

$$F = \frac{2}{3}\frac{m_e\mu_0^2}{\hbar^2 e^2}\left\langle G\left|\sum_i\left[\hbar\omega_0 - \lambda\left(\hat{a}_i^\dagger + \hat{a}_i\right)\right](1 - 2\hat{n}_i)\right|G\right\rangle. \quad (15)$$

We explicitly verified that the total oscillator strength calculated for the complete model as the sum of the oscillator strengths of the individual transitions coincided with the ground state expectation value in the above equation. The vibrational contribution in the above expression simply renormalizes the bare exciton frequency, $\hbar\omega_0$, a marginal correction

as the ground state expectation value of $(\hat{a}_i^\dagger + \hat{a}_i)$ is negligible. Neglecting this correction, the oscillator strength F in eqn (15) is made up of two terms: the first term coincides with the oscillator strength of N non-interacting molecules (see eqn (1)), while the second term describes the correction to the oscillator strength due the finite weight in the ground state of states with a finite exciton number. We stress that the HL approximation leads in the standard exciton model to sizable deviations of absorption intensity from exact results already for J values one order of magnitude smaller than the unperturbed exciton frequency. This very general result must be accounted for when addressing hypo- and hyperchromism in molecular aggregates: relaxing the HL approximation in fact naturally explains hyperchromic effects in J-aggregates and hypochromic effects in H-aggregates.

Calculated emission spectra for the same systems as in Fig. 2 are shown in Fig. 3 (results for long-range intermolecular interactions and for different values of λ are shown in the ESI†). The intensity of the emission for H aggregates is lower than that of J-aggregates by more than two orders of magnitude (of course we are referring to the nominal fluorescence intensity, not taking into account non-radiative deactivation pathways). As it is well known, the fluorescent state in H-aggregate is in the $K = K_{max}$ subspace and is therefore a dark state. Indeed it acquires a finite (albeit weak) intensity due to vibronic coupling and, specifically, due to the presence of $K = K_{max}$ states in the vibrational manifold of the ground state. Because the zero-phonon line is forbidden by symmetry, the H-aggregate emission is even more red-shifted than the emission of the J-aggregate. As for the quality of the results obtained in the HL approximation, the position and shape of the fluorescence band are well approximated while, in line with the above discussion, the emission intensity is overestimated for H-aggregates and underestimated for J-aggregates.

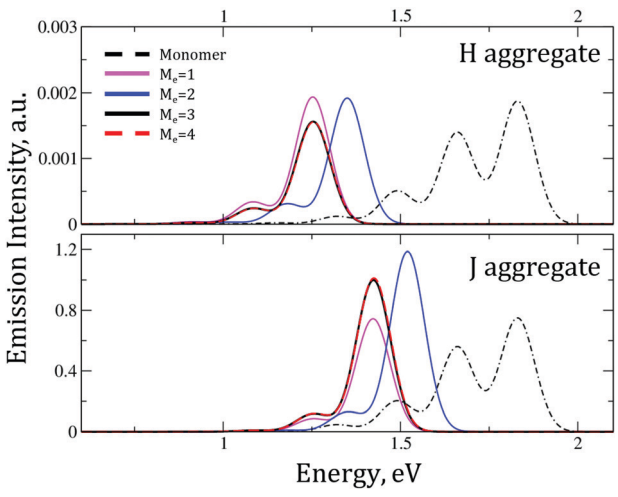

Fig. 3 Emission spectra calculated for the same system as in Fig. 2. In the upper panel, the monomer emission intensity is rescaled by a factor of 1/400 in order to maintain it comparable to the very weak intensity calculated for the H-aggregate.

5 Testing approximation schemes

Exact diagonalization approaches are limited to small aggregates, up to 7 sites for the complete model and up to 10 sites in the HL approximation. The electronic basis is comparatively small, growing with N in the HL approximation and as 2^N in the complete model. Indeed the basis blows up because of the vibrational states: accounting for just three vibrational quanta per site would multiply by a 3^N factor the basis dimension. It is therefore very important to discuss approximation schemes to cut the basis dimension and particularly so for vibrational states. Indeed the HL electronic basis is already very small, and we already discussed how the electronic basis in the complete model can be reduced by fixing a maximum number of excitons ($M_e = 3$ seems to work pretty well in most cases of interest in this study, even if this approximation is untenable for clusters of polar and polarizable dyes[18,20]).

Recently,[20] discussing J-aggregates of polar dyes, we realized that for largely delocalized excitons only the vibrational modes in the close proximity of the center of the Brillouin zone are effectively coupled to the electronic degrees of freedom so that, instead of accounting for N local harmonic oscillators, reasonable results are obtained accounting for the single oscillator with $q = 0$. This of course leads to an enormous reduction of the basis dimension. The Hamiltonian in eqn (8) shows that accounting for just the $q = 0$ mode one obtains a similar coupling Hamiltonian as for the isolated molecule, but with the strength of the coupling reduced to $\lambda/\sqrt{N}$. As a result, in this approximation the same bandshape is calculated for J and H aggregates, as shown in the top panels of Fig. 4, where we show absorption spectra calculated in the HL approximation for the same model parameters as in Fig. 2. A full decoupling of the $q = 0$ vibrational mode is expected in the infinite chain limit, but also in these conditions a finite vibronic structure is

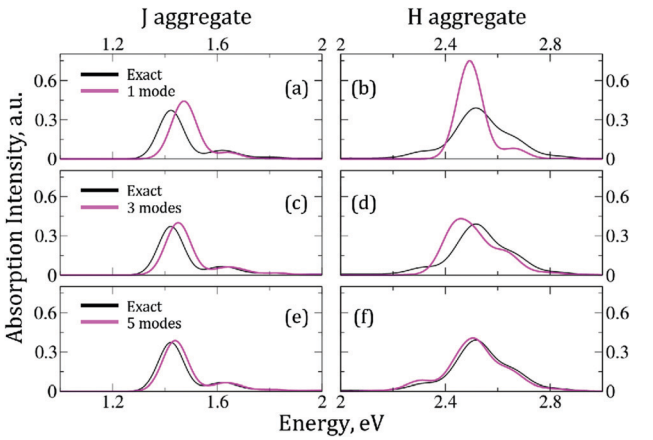

Fig. 4 Calculated absorption spectra for J and H aggregates (left and right panels, respectively) calculated in the HL approximation for the same model parameters as in Fig. 2. Results refer to aggregates of 10 molecules, black lines show numerically exact results, obtained with $M_v = 4$, magenta lines show results calculated only accounting for the $q = 0$ mode (a and b), $q \in \left\{-\frac{\pi}{5}, 0, \frac{\pi}{5}\right\}$ (c and d), $q \in \left\{-\frac{2}{5}\pi, -\frac{\pi}{5}, 0, \frac{\pi}{5}, \frac{2}{5}\pi\right\}$ (e and f).

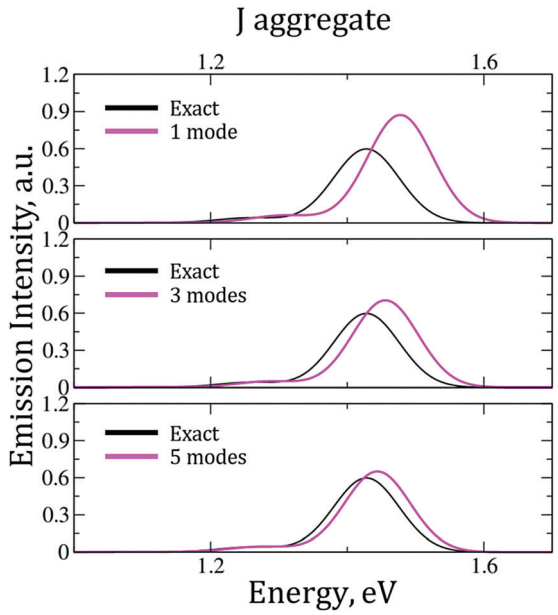

Fig. 5 Emission spectra calculated for the same system as in left panel of Fig. 4.

observed due to the coupling to modes with finite q.[12] Indeed, adding the two nearest modes to the $q = 0$ mode in the Brillouin zone (middle panels of Fig. 4) improves the agreement and adding 2 more modes (for a grand total of 5 delocalized vibrations, bottom panels) gives very good results for J aggregates and an acceptable agreement for H-aggregates. Similar results are obtained for emission spectra in Fig. 5. Cutting vibrational modes in the Fourier space works in principle for the complete as well as for the standard exciton model, but, apart from the simplest case where only the $q = 0$ mode is accounted for, the approach is difficult to implement in the complete model. Moreover this approximation is expected to work well for largely delocalized excitons. Of course for localized excitons or in the presence of disorder the approach could only work if many modes (possibly all) in the reciprocal space are introduced, making the approximation useless.

A useful and widely adopted approach to the reduction of the vibrational space is the so-called few-particle approximation.[32,33] The two particle approximation (2PA) was validated against exact diagonalization results in a square lattice,[34] and, together with its extended version, the three particle approximation (3PA), was extensively applied by Spano.[11,12] Few particle approximations work in the real space, so that they do not require a symmetric or ordered system, but only apply in the HL approximation where all relevant basis states have a single exciton. In the 2PA approximation, the basis is cut imposing a maximum number n_e of vibronic excitations on the electronically excited states (notice that these vibronic states refer to the displaced harmonic oscillator as relevant to the electronically excited state). Moreover a maximum number of vibrational quanta n_v can be present in just a single additional site, different from the site bearing the exciton. In the three particle approximation (3PA), one accounts for vibrational excitations occurring on up to two sites.

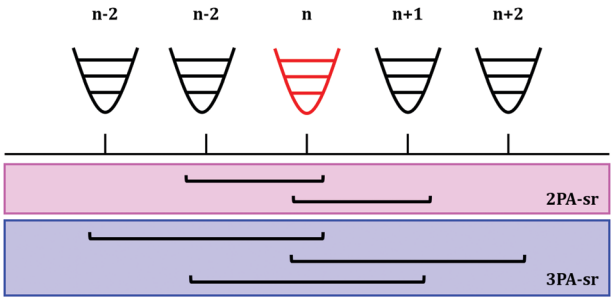

Fig. 6 Scheme representing the allowed combination of states allowed in the sr ansatz. The red oscillator represents the vibronically excited state.

Two different approximation schemes are possible for both 2PA and 3PA, a short-range (sr) scheme, where vibrational excitations are only allowed in the nearest sites of the site bearing the exciton (Fig. 6), or a long-range (lr) scheme, where vibrational sites can be spread all over the aggregate. Of course the 2PA-sr or the 3PA-sr only apply when the exciton model accounts for nearest neighbor interactions, while one must resort to lr-schemes when accounting for long-range electrostatic interactions. To be specific, the 2PA basis set is:

$$|\psi_{2PA}\rangle = |n,\tilde{\nu},\nu_l\rangle, \quad l \neq n, \tag{16}$$

where n marks the site where the exciton resides and $\tilde{\nu}$ counts the number of vibrational quanta in the displaced oscillator associated with the same site. The numbers $\nu_{l\neq n}$ count the vibrational quanta in the undisplaced harmonic oscillator on site l. In the sr flavor of 2PA, $l = n \pm 1$, while in the lr flavor, l can assume any value different from n. The diagonal energy of the 2PA states is easily calculated as $\hbar\omega_0 + (\tilde{\nu} + \nu_l)\hbar\omega_v$. Off diagonal matrix elements, accounting for the interaction between different sites, are:

$$\langle n,\tilde{\nu},\nu_l|\hat{H}|m,\tilde{\mu},\mu_k\rangle = J_{m-n} f_{\tilde{\nu},\mu_n} f_{\tilde{\mu},\nu_m} \prod_{i\neq n,m} \delta_{\nu_i,\mu_i}, \tag{17}$$

where $f_{\tilde{\nu},\mu_m}$ is the Franck–Condon factor measuring the overlap between the $\tilde{\nu}$ vibronic level of excited state and μ vibrational level. Finally, the transition dipole moment is calculated as follows:

$$\mu_i^{\text{trans}} = \langle G|\hat{\mu}|\psi_i\rangle = \sum_{n,\tilde{\nu}} c_{n,\tilde{\nu}} \langle G|\hat{\mu}|n,\tilde{\nu},0\rangle = \sum_{n,\tilde{\nu}} c_{n,\tilde{\nu}} \mu_0 f_{\tilde{\nu},0}. \tag{18}$$

Moving to the 3PA, the relevant basis set reads $|\psi_{3PA}\rangle = |n,\tilde{\nu},\nu_l,\nu_{l'}\rangle$, $l,l' \neq n$. Accordingly, the diagonal energy is $\hbar\omega_0 + (\tilde{\nu} + \nu_l + \nu_{l'})\hbar\omega_v$, while the Hamiltonian off-diagonal matrix elements are:

$$\langle n,\tilde{\nu},\nu_l,\nu_{l'}|\hat{H}|m,\tilde{\mu},\mu_k,\mu_{k'}\rangle = J_{m-n} f_{\tilde{\nu},\mu_n} f_{\tilde{\mu},\nu_m} \prod_{i\neq n,m} \delta_{\nu_i,\mu_i}. \tag{19}$$

Fig. 7 compares absorption spectra calculated *via* exact diagonalization and with the 2PA-sr and 3PA-sr for an aggregate of 10 molecules, described by the standard exciton model, with increasing strength of nearest-neighbor interactions, J. For J-aggregates the 2PA and 3PA approximations work pretty well up to medium-large interactions, but for H-aggregates, having a

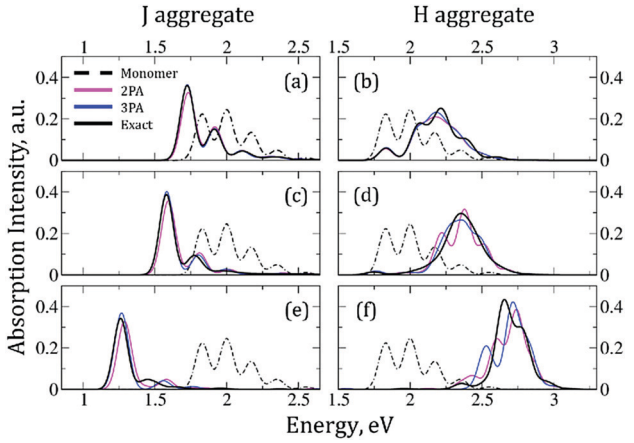

Fig. 7 Absorption spectra for aggregates of 10 molecules in the HL approximation and only accounting for nearest neighbor interactions. Exact results are compared with results obtained in the 2PA-sr and 3PA-sr approximations. The maximum number of vibrational quanta is fixed to 6. Dashed lines refer to the monomer limit. Model parameters are fixed at $\hbar\omega_0 = 2.0$ eV, $\lambda = 0.17$ eV, $\hbar\omega_v = 0.17$ eV. In left panels (J-aggregates) J varies from -0.085 eV (a) to -0.17 eV (c), and -0.34 eV (e). In the right panels (H-aggregates) it varies from 0.085 eV (b), 0.17 eV (d), 0.34 eV (f).

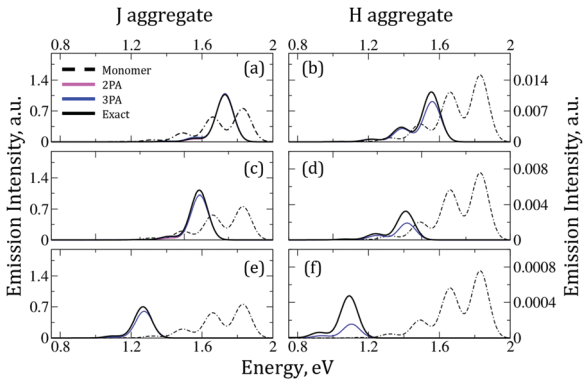

Fig. 8 Emission spectra for 2PA-sp, 3PA-sp and exact excitonic models. Same parameters as in Fig. 7. For H-aggregates (right panels) the intensity of the monomer spectrum is rescaled by a factor 1/50 (panel b), 1/100 (panel d) and 1/1000 (panel f).

much more complex spectral shape, the approximation is poor already for interactions of medium strength. Similar results hold true for emission spectra in Fig. 8. Moving to 2PA-lr or 3PA-lr does not change the picture (see ESI†), as expected.

The lr extensions of the 2PA and 3PA approaches has to be invoked for systems where long-range Coulomb interactions are accounted for. However the 3PA-lr basis is very large, making it impossible to deal with aggregates with more than 6 sites. Therefore Fig. 9 and 10 compare exact and 2PA-lr results for absorption and emission spectra, respectively, of 10 site aggregates with long-range intermolecular interactions.

6 Conclusions

Electrostatic intermolecular interactions and molecular vibrations govern the spectral properties of molecular aggregates

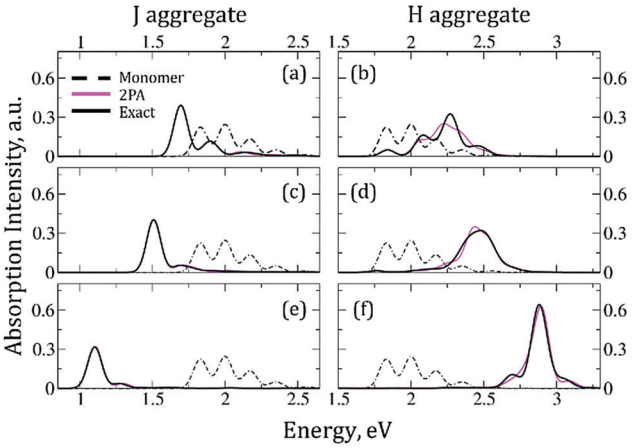

Fig. 9 Results for the same systems as in Fig. 7 but accounting for long-range interactions.

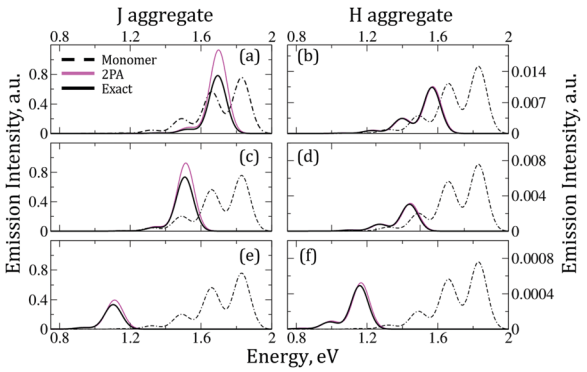

Fig. 10 Emission spectra for 2PA-lr and exact excitonic models. Same parameters as in Fig. 9. For H-aggregates (right panels) the intensity of the monomer spectrum is rescaled by a factor 1/50 (panel b), 1/100 (panel d) and 1/1000 (panel f).

and crystals, leading to a complex, intrinsically non-adiabatic problem. Even in the simplest systems where the high molecular symmetry and the comparatively large intermolecular distances reduce intermolecular interaction to the interactions between transition dipole moments, several approximations are usually adopted to make the model tractable. In this work a clever use of translational symmetry allowed us to obtain numerically exact results for aggregates of sizable dimensions, that were used to validate several approximation schemes. The first and most important approximation is the widespread HL approximation that, neglecting the interactions that mix non-degenerate states, leads to the standard exciton model, as usually adopted for either molecular crystals or aggregates. The approximation leads, by error cancellation, to a good estimate for the spectral frequency and bandshape, but it fails to reproduce the spectral intensity. Indeed the standard exciton model, due to the HL approximation, breaks the fundamental sum rule for the oscillator strength. Spectral intensities are underestimated by the standard exciton model for J-aggregates and overestimated for H-aggregates, with effects that, increasing with the strength of intermolecular interactions, are already

sizable for intermolecular interactions one order of magnitude smaller than the molecular excitation energy. Unfortunately, the dimension of the basis for the complete model is very large and even if translational symmetry is exploited to reduce the dimensions of the matrices to be diagonalized, we were not able to deal with aggregates composed by more than 6–7 molecules.

If we are not interested in the precise estimate of the spectral intensity, the HL approximation is fairly safe and considerably reduces the dimension of the problem. *Via* a clever use of translational symmetry, we obtained numerically exact results on aggregates with up to 10 molecules. For systems where just nearest neighbor interactions enter into play, the two and three-particle approximations, restricted to nearest neighbor particles offer a convenient way to obtain reliable results for J-aggregates and reasonable results for H-aggregates. If long-range interactions are of interest, the short range version of the two- and three-particle approximations must be abandoned and the particles can be located at any distance. This leads to extremely large basis for the three-particle approximation, that becomes more expensive than the exact diagonalization. However in this case the 2PA already leads to good results for both J and H-aggregates.

Moving from one-dimension to two-dimensions, as relevant to many organic crystals where sizable interactions are only found along preferential directions defining 2D lattices,[12,34,35] is an additional challenge, mainly because of the need to consider bigger aggregates. The 2PA and 3PA basis grow quite impressively when going from 1D to 2D. Instead symmetry can be implemented quite naturally in 2D systems, leading to basis dimensions that are the same as for 1D aggregates composed of the same number of molecules.

Conflicts of interest

There are no conflicts to declare.

Acknowledgements

The authors gratefully acknowledge financial support from the Italian Ministero dell'Istruzione, dell'Università e della Ricerca (MIUR): grant Dipartimenti di Eccellenza (DM 11/05/2017 no. 262). This project has received funding from the European Union Horizon 2020 research and innovation programme under grant agreement no. 812872 (TADFlife). This research benefits from the HPC (High Performance Computing) facility of the University of Parma, Italy.

Notes and references

1 R. S. Mulliken, *J. Am. Chem. Soc.*, 1952, **74**, 811–824.
2 Z. G. Soos and D. J. Klein, *Molecular Association: Including Molecular Complexes*, Academic Press, New York, 1975, vol. 1.
3 M. J. Rice, *Phys. Rev. Lett.*, 1976, **37**, 36–39.
4 A. Painelli and A. Girlando, *J. Chem. Phys.*, 1986, **84**, 5655–5671.
5 L. Del Freo, A. Painelli and Z. G. Soos, *Phys. Rev. Lett.*, 2002, **89**, 027402.
6 G. D'Avino, M. Masino, A. Girlando and A. Painelli, *Phys. Rev. B: Condens. Matter Mater. Phys.*, 2011, **83**, 161105.
7 Th. Förster, in *Modern Quantum Chemistry*, ed. O. Sinanoglu, Academic Press, 1965, p. 93.
8 G. D. Scholes, *Annu. Rev. Phys. Chem.*, 2003, **54**, 57–87.
9 F. Di Maiolo and A. Painelli, *J. Chem. Theory Comput.*, 2018, **14**, 5339–5349.
10 J. Knoester, in *Organic Nanostructures: Science and Applications*, ed. G. C. La Rocca and V. M. Agranovich, IOS Press, Amsterdam, 2002, vol. 149, pp. 149–186.
11 F. C. Spano, *Acc. Chem. Res.*, 2010, **43**, 429–439.
12 N. J. Hestand and F. C. Spano, *Chem. Rev.*, 2018, **118**, 7069–7163.
13 D. P. Craig and S. H. Walmsley, *Excitons in Molecular Crystals*, Benjamin, 1968.
14 A. S. Davidov, *Theory of Molecular Excitons*, Plenum Press, 1971.
15 V. M. Agranovich and M. D. Galanin, *Excitons in Molecular Crystals*, North-Holland, 1982.
16 E. E. Jelley, *Nature*, 1936, **138**, 1009–1010.
17 M. Kasha, *Radiat. Res.*, 1964, **3**, 317–331.
18 F. Terenziani and A. Painelli, *Phys. Rev. B: Condens. Matter Mater. Phys.*, 2003, **68**, 165405.
19 F. Terenziani, G. D'Avino and A. Painelli, *ChemPhysChem*, 2007, **8**, 2433–2444.
20 S. Sanyal, C. Sissa, F. Terenziani, S. K. Pati and A. Painelli, *Phys. Chem. Chem. Phys.*, 2017, **19**, 24979–24984.
21 G. D'Avino, F. Terenziani and A. Painelli, *ChemPhysChem*, 2007, **8**, 2433–2444.
22 S. Sanyal, A. Painelli, S. K. Pati, F. Terenziani and C. Sissa, *Phys. Chem. Chem. Phys.*, 2016, **18**, 28198–28208.
23 B. Bardi, C. Dall'Agnese, M. Tassé, S. Ladeira, A. Painelli, K. I. Moineau-Chane Ching and F. Terenziani, *ChemPhotoChem*, 2018, **2**, 1027–1037.
24 C. Zheng, C. Zhong, C. J. Collison and F. C. Spano, *J. Phys. Chem. C*, 2019, **123**, 3203–3215.
25 S. Paganelli and S. Ciuchi, *J. Phys.: Condens. Matter*, 2006, **18**, 7669–7685.
26 S. Paganelli and S. Ciuchi, *J. Phys.: Condens. Matter*, 2008, **20**, 235203.
27 B. Bardi, C. Dall'Agnese, K. I. Moineau-Chane Ching, A. Painelli and F. Terenziani, *J. Phys. Chem. C*, 2017, **121**, 17466–17478.
28 J. R. Lakowicz, *Principles of Fluorescence Spectroscopy*, Springer US, 1999, p. 698.
29 V. M. Agranovich and B. S. Toshich, *Soviet Physics JETP*, 1968, **26**, 149–162.
30 F. C. Spano and H. Yamagata, *J. Phys. Chem. B*, 2011, **111**, 5133–5143.
31 C. Sissa, A. Painelli, M. Blanchard-Desce and F. Terenziani, *J. Phys. Chem. B*, 2011, **115**, 7009–7020.
32 M. R. Philpott, *J. Chem. Phys.*, 1971, **55**, 2039–2054.
33 M. Hoffmann and Z. G. Soos, *Phys. Rev. B: Condens. Matter Mater. Phys.*, 2002, **66**, 024305.
34 F. C. Spano, *J. Chem. Phys.*, 2002, **116**, 5877–5891.
35 Z. Zhao and F. C. Spano, *J. Chem. Phys.*, 2005, **122**, 114701.

